International Information and Engineering Technology Association

Mathematical Modelling of Engineering Problems
Vol. 12, No. 3, March, 2025, pp. 797-806
Journal homepage: http://iieta.org/journals/mmep

Evaluation of Surface Texture of Hydrogen Pressure Regulators

Miroslav Hristov Hristov

Technical College – Sofia, Technical University of Sofia, Sofia 1756, Bulgaria

Corresponding Author Email: miro.hr@tu-sofia.bg

https://doi.org/10.18280/mmep.120306

Received: 4 January 2025
Revised: 5 March 2025
Accepted: 10 March 2025
Available online: 31 March 2025

Keywords:
surface texture, surface roughness, hydrogen (H_2), hydrogen pressure regulators

ABSTRACT

As a prospective fuel source, hydrogen presents a series of technological challenges that must be overcome to ensure its effective utilization. A critical component in hydrogen systems is the pressure regulator, which functions by reducing the high inlet pressure to levels that are more than ten times lower than the outlet pressure. Pressure regulators for hydrogen are essential to guarantee high efficiency and reliable operation of the hydrogen fuel cell. The achievement of the technical parameters of the regulators is contingent on specific requirements concerning surface geometry and surface texture parameters, which are a consequence of the characteristics of the hydrogen molecule. Through a thorough analysis of the surface texture parameters, it is possible to ensure smoother, reliable and long-life operation. Statistical mathematical methods can bring about a reduction of the geometric control requirements of the surfaces of critical elements of hydrogen pressure regulators. The control of surface roughness in specific areas, tailored to the technological and design features of the pressure regulators, can ensure the smooth operation of the various hydrogen fuel systems in which it is applied and affect the manufacturing process.

1. INTRODUCTION

Driven by recent technological advances and the growing need for diverse and sustainable technologies, particularly in the oil-consuming transport sector, governments are focusing their R&D efforts on hydrogen and fuel cells. Fuel cells are a major focus, but technologies for the production, storage, transport and use of hydrogen should not be neglected [1].

Fuel-cell-powered vehicles have the potential to significantly improve fuel economy and reduce emissions. Fuel cell-based vehicles are classified as fuel cell-ICE hybrid vehicles (FCIHVs) and fuel cell-battery hybrid vehicles (FCHVs), the former refers to the evolution from the existing ICE-battery hybrid vehicles (IBHVs) to the latter, which is also occasionally known as fuel cell vehicles (FCVs) [2].

Hydrogen has some undeniable advantages over fossil fuels in terms of the absence of greenhouse gases in use, production from renewable energy sources, flexibility in sources, flexibility in energy transmission, production and storage. Unfortunately, hydrogen has high production costs. Its low density leads to problems with storage and transmission, which requires very high pressure [3, 4].

The utilization of hydrogen in operational contexts is associated with a number of challenges, primarily related to the unique properties of the hydrogen molecule. Due to its relatively small size, hydrogen is inherently difficult to seal, and it reacts with numerous materials commonly used in industrial applications, potentially compromising their inherent properties. This necessitates the use of specialized materials and coatings to ensure the safe and effective integration of hydrogen into industrial processes.

The specific characteristics and chemical properties of hydrogen require the implementation of specific design solutions and the appropriate selection of materials to ensure the effective functioning of hydrogen fuel systems their mission critical elements.

The construction of hydrogen fuel systems entails the incorporation of several pivotal components that collectively influence the system's overall efficiency, reliability, and safety. Among these components is the pressure regulator, which is tasked with reducing the pressure from P_{in} (inlet pressure) 35/70 MPa to 1/1.5 MPa or less P_{out} (outlet pressure). This reduction is essential for ensuring the optimal functioning of the downstream components, including the hydrogen fuel cell and its associated applications.

In order to guarantee the functionality and safety of hydrogen pressure regulators, it is vital to address one of the primary challenges associated with the handling of hydrogen (H_2) – specifically, the issue of leakage to the atmosphere [4]. This necessitates the implementation of specific requirements pertaining to the sealing of both static and dynamic connections, ensuring that the requisite surface geometry and surface roughness requirements are met.

2. PRESSURE REGULATORS AS PART OF THE HYDROGEN FUEL SYSTEM

At the present time, the primary application of hydrogen fuel systems is in the automotive industry, where hydrogen fuel cell electric vehicles (FCEVs) are capable of achieving zero exhaust emissions and zero pollution [5].

The FCV is regarded as a significant zero-emission alternative, presenting a range and refueling time comparable to that of internal combustion engine vehicles. A multitude of model-based studies have been conducted with the objective of enhancing fuel cell system and management in automotive applications. One of the principal components of the fuel system is the pressure regulator, which has a considerable influence on the overall performance of the automotive powertrain (Figure 1) [6].

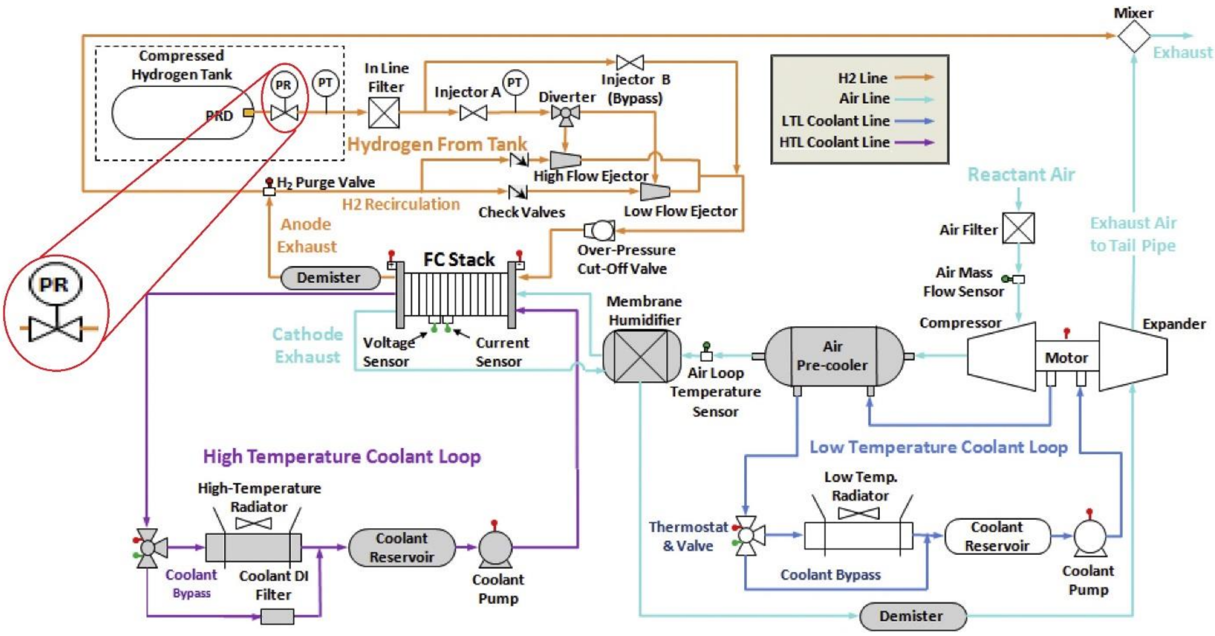

Figure 1. Pressure regulator as a part of the hydrogen supply system in the LDV automotive fuel cell system [7]

The efficacy of the system is contingent upon the functionality of the pressure-regulating components, which are responsible for ensuring the optimal delivery of hydrogen at a specified pressure [6].

A hydrogen FCEV is capable of achieving effectively zero exhaust emissions and zero pollution. It is not only an optimal substitute for conventional FCVs, but also the principal method of utilizing hydrogen energy in an efficient manner [8]. The primary method of providing mileage comparable to that of conventional internal combustion engine vehicles is through the utilization of high-pressure hydrogen storage. This necessitates that the hydrogen within the gas cylinder be maintained at a pressure of 30-35 MPa [9]. The typical operational pressure of a proton exchange membrane hydrogen fuel cell is 0.16 MPa. Accordingly, a pressure reduction system has been devised for the FCEV. In consideration of the thermodynamic properties of hydrogen, a two-stage pressure reduction method is currently employed for the FCEV. The two-stage process entails a reduction in pressure from 35 MPa to 5 MPa in the initial stage and from 5 MPa to 0.16 MPa in the subsequent stage [5].

In a hydrogen power system, an increase in pressure can result in enhanced corrosion of the cathode, which may ultimately culminate in a short circuit within the cell and reduced efficiency or inoperability. Accordingly, the pressure selected for supplying the fuel cell with hydrogen has a direct correlation with the cell's lifespan, fuel consumption, and the commercial viability of the system [10].

The considerable difference between inlet and reduced pressure levels gives rise to the specific operation of the regulators, which in turn necessitates particular requirements for the geometry and surface roughness of the components, as well as the utilization of materials that are conducive to the sealing of the hydrogen molecule.

3. HYDROGEN PRESSURE REGULATOR INFORMATION

The design, technology and metrology of hydrogen pressure regulators are specific to their intended application, performance and technical parameters.

The functional specifics of the RH242 hydrogen pressure regulators (Figure 2) also determine a number of technological specifics. Due to the high-pressure conversion ratio of P_1= 35(70) MPa (reduced pressure from the first stage of the pressure regulator) to P_2 values around 2.5 MPa (reduced pressure from the second stage of the pressure regulator), specific design solutions are utilized in the regulators.

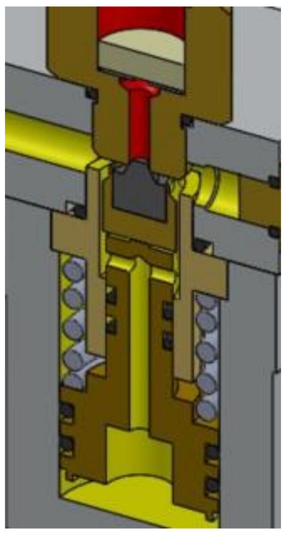

Figure 2. CAD model module of the initial reduction stage of the hydrogen pressure regulator RH242, as by Memtex [11]

If we ignore the effects of friction and deformation on the conversion function and consider them as sources of variability in the output pressure, we obtain the following pressure reduction function for the first stage (P_1) of RH242:

$$\Delta P = P_{in} - P_1 = f\left(\frac{d}{dy_1}, S_1, \frac{F_{P_{in}}}{F_{sp1}}\right) \quad (1)$$

where, y_1 – moving the piston of the first stage; S_1 – piston area of the first stage; F_{Pin} – pressure force on the piston of the first stage; F_{sp1} – spring force of the first stage.

In the first stage, we have a change of the transition cross section S_1 as a function of the piston displacement y_1:

$$\Delta y_1 = 0.1 \div 0.2 \text{ mm} \quad (2)$$

The relatively small displacements of the piston in the first stage of the hydrogen pressure regulator result in specific requirements for the cylinder shape deviation due to the significant ratio between the piston diameter (D_1) and its relative displacement (Δy_1) during operation:

$$\frac{\Delta y_1}{D_1} \ll 1 \quad (3)$$

Consequently, it is not necessary to control the cylindricity deviation (Figure 3) along the entire length of the cylinder; instead, the measurement of the roundness deviation in two sections within the piston working area is sufficient.

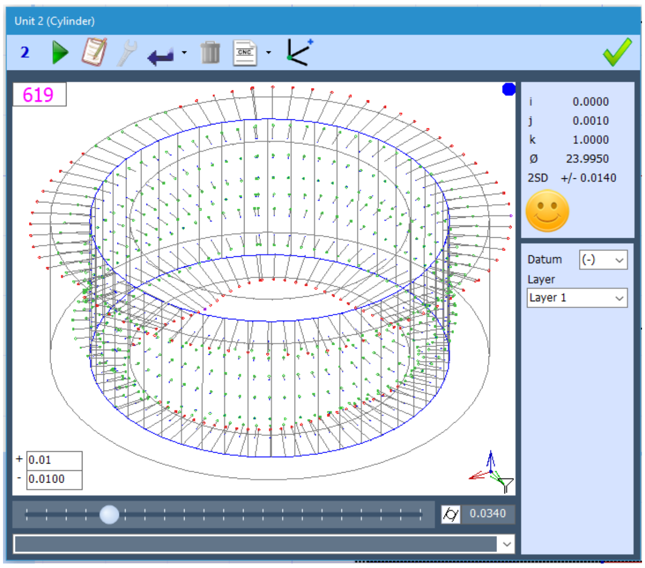

Figure 3. Visual representation of cylindricity deviation measurement of RH242 regulator element with CMM Aberlink Horizon [12]

As demonstrated in the case of the operation of pressure regulators from different manufacturers (see Figure 4), similar small deviations can be observed. These specific design solutions are indicative of the manufacturers' know-how related to the technological and production process, and these characteristics are also directly linked to the choice of material for hydrogen pressure regulators, the possibilities and ways of surface treatment to achieve the technical parameters. The different coatings for the different materials should not be overlooked, as they have a significant influence on both the geometry of the surfaces and the surface texture parameters.

The selection of materials for the various components of the hydrogen system, including pressure regulators, requires careful consideration. The hydrogen molecule is notably small, which enables it to penetrate materials that are impermeable to other gases. Furthermore, the hydrogen molecule is capable of dissociating on the surface of the material, which can have a detrimental impact on its mechanical characteristics. Additionally, cracks or other defects may occur. This phenomenon is well documented and is referred to as hydrogen embrittlement [13, 14].

To mitigate the adverse effects of hydrogen, the use of certified materials or suitable coatings is recommended.

The selection of materials for hydrogen pressure regulators is of critical importance due to the unique challenges posed by hydrogen. The main requirements for the materials are that they are lightweight, durable, and corrosion-resistant. For components that are subjected to high loads due to the high pressure (700 bar), the use of Stainless Steel (316/316 L) is appropriate. The properties of this material include excellent resistance to hydrogen embrittlement, corrosion resistance, and high strength. Another material with suitable characteristics is Titanium Alloys (Grade 5, Ti-6Al-4V), which, when compared to Stainless Steel, is significantly lighter while maintaining a high strength-to-weight ratio and good resistance to hydrogen embrittlement. A major disadvantage of Titanium Alloys is the relatively high cost. Conversely, Aluminium Alloys can be utilized for elements not subjected to high loads and pressures, thereby reducing the overall weight of pressure regulators. The utilisation of different coatings is a viable method to enhance the properties of metal materials. For instance, Electroless Nickel Plating can be employed to augment corrosion resistance and mitigate hydrogen permeation, while Ceramic Coatings can be used to enhance wear resistance and thermal insulation. Anodising can be employed to enhance the properties of aluminium alloys, thereby achieving higher hydrogen resistance and wear resistance. Anodised Aluminium T6511 is a prime example of this.

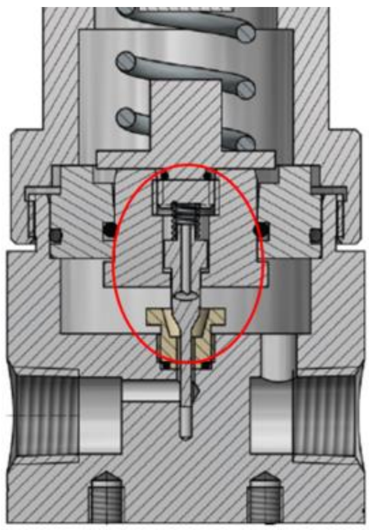

Figure 4. CAD model of the hydrogen back pressure regulator Pressure Tech BP301 [15]

It is imperative to note that other critical elements of pressure regulators include seals, which are essential for ensuring airtightness and preventing internal and external leakages. Hydrogen-compatible elastomers and polymers are predominantly utilized to provide low friction and excellent chemical resistance, in addition to minimising hydrogen permeation in sealing applications (e.g. O-rings) and wear-resistant components (e.g. PTFE (Teflon) or PEEK). The materials used for elements of static and dynamic seals in low-pressure sections or as secondary seals include Viton (FKM/FPM) or EPDM, which exhibit excellent flexibility, chemical resistance, and low hydrogen permeation.

The specific functionality and technological solutions related to the mechanical design of the hydrogen pressure regulators determine the relatively small piston displacements, which allows the definition of the surface texture requirements.

The requirements for profile, waviness and roughness can be applied in a small measurement area, which is sufficient to ensure that no hydrogen leaks into the atmosphere. Furthermore, smooth piston movement and a correspondingly smooth performance characteristic will be ensured, as well as high wear resistance at the contact between metallic and non-metallic materials.

4. SURFACE ROUGHNESS TEXTURE

The continuous increase in demand for improved reliability and mechanical parts, coupled with a reduction in frictional losses and, in particular, an increase in power density, is resulting in a notable rise in the tribological load on contact surfaces. The characteristics of the contact between the surfaces in question are becoming increasingly significant. Two of the most crucial surface properties are surface roughness and topography (Figure 5). For the optimal design of contact surfaces, it is of paramount importance to comprehend the impact of surface roughness parameters on friction, wear and tear, particularly in the context of hydrogen systems [16].

The experimental setup for measuring the roughness and topography of a Memtex RH242 hydrogen pressure regulator is presented in Figure 5. The measurement was performed with a Taylor Hobson Form Talysurf i-Series. The graphical results of the roughness parameter measurement (Graphic 1) and the profile parameters (Graphic 2) are presented, with additional lines located at 11.5 mm and 13.5 mm showing an area with a profile close to linear, which reflects the piston working area. The graphical results thus presented justify the need for increased control of surface texture parameters, at the expense of less tight control of surface shape deviation.

In order to ascertain the primary surface characteristics of the critical elements of the Memtex RH242 hydrogen pressure regulators [11], the surface texture and topography parameters have been measured using the Taylor Hobson Form Talysurf i-Series [17]. Based on the preliminary observations, the surface roughness parameters have been selected for control, and the data has been statistically processed and analyzed.

A number of different surface roughness parameters may be utilized, depending on the specific circumstances. These characteristics are associated with the geometrical properties of the workpiece. These parameters are defined and can be found in several standards, including ISO 4287:1997 [18], ISO 1302:2003 [19], and ISO 21920:2021 [20]. The selection of an appropriate measurement parameter is crucial for the accurate determination of roughness. The surface parameters can be calculated from the filtered roughness profile. The most commonly utilized surface parameters are outlined below [21].

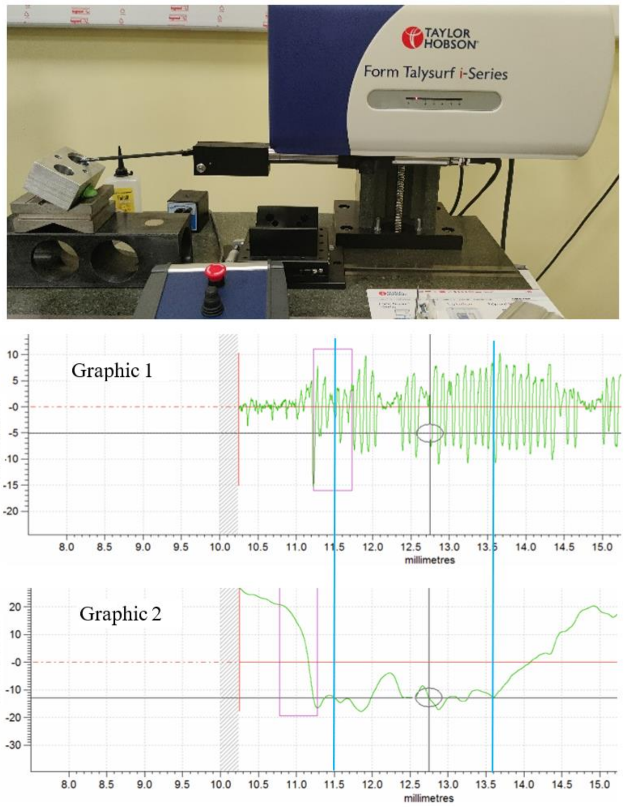

Figure 5. Experimental installation and measurement results of roughness and topography for Memtex RH242 hydrogen pressure regulator using Taylor Hobson Form Talysurf i-series [22]

The arithmetic mean of the absolute ordinate values, $Z(x)$, within the sampling length is defined as Ra (Eq. (4) [18]). It is important to note that this roughness parameter of a surface can vary considerably without affecting the performance of the surface. Therefore, it is common practice to specify a tolerance band or a maximum Ra value that is acceptable on the drawing [23]:

$$Ra = \frac{1}{l}\int_0^l |Z(x)|dx \tag{4}$$

The Ra value for a given sample length represents the average roughness, and thus the effect of an atypical peak or valley will have only a minor influence on the value. It is recommended that the Ra value be estimated for several successive sampling lengths and the resulting values averaged. This will ensure that the Ra value is representative of the surface being inspected. It is essential that the measurements be made perpendicular to the surface. The Ra value does not provide information about the shape of irregularities on the surface. Similar Ra values can be obtained for surfaces with markedly different profiles. It is useful to indicate the machining process used to produce the surface [23].

As the requirements for surface texture have evolved, so have the standards. The most significant change in ISO 21920 [20] concerns the manner in which the calculation is conducted, it is no longer performed repeatedly and subsequently averaged. The revised calculation method entails a single value of Ra (or Rq). However, this does not apply to Rp, Rv and Rz, which continue to be averaged to minimize the impact of outliers [24].

Rq (Eq. (5) [18]) is the root mean square value of the ordinate values *Z*(*x*) within the sampling length and expressed mathematically [23]:

$$Rq = \sqrt{\frac{1}{l}\int_0^l Z^2(x)dx} \tag{5}$$

When compared to the arithmetic average, the root mean square parameter has the effect of giving extra weight to the numerically higher values of surface height [23].

When roughness parameters are determined instrumentally *Rq* has the advantage that phase effects from electrical filters can be neglected. The *Ra* parameter using the arithmetic average is affected by phase effects that cannot be ignored. *Ra* has almost superseded *Rq* on machining specifications. However, *Rq* still has value in optical applications where it is more directly related to the optical quality of a surface [23].

Rz, the maximum height of the profile is defined in accordance with the sampling length. This parameter is frequently used to ascertain whether the profile exhibits protruding peaks that may potentially impact the static or sliding contact function [18, 25].

The different ISO standards provide a variety of definitions and methodologies for calculating the *Ra* parameter.

Rt (Eq. (6)), (total height of the profile) is parameter that highly susceptible to the influence of elevated peaks or deep scratches. The *Rt* value is defined as the vertical distance between the highest peak (*Rp*) and the lowest valley (*Rv*) along the specified assessment length of the profile [18, 26].

$$Rt = maxRp_i + maxRv_i \tag{6}$$

Rp (Eq. (7)), maximum profile peak height: height of the highest peak from the mean line, defined on the sampling length [18, 25].

Use a natural cubic spline to interpolate through the discrete data values. For each sample length *i*=1 to *CN*. Determine portions of the profile above the mean line, these are the profile peaks. For each profile peak *j*=1 to *m*, determine the supremum height Z_{pj}:

$$Rp = \frac{1}{CN}\sum_{i=1}^{CN} Rp_i \tag{7}$$

where,

$$Rp_i = \max_{1\leq j\leq m} Zp_i \tag{8}$$

In many tribological applications, *Rp* and *Ry* is an important parameter because damage may be done to the interface by the few extreme deviations from the mean line [27]. Highest peak and the lowest valley (*Rv*) may affect smooth translation or the isolation of hydrogen from the environment.

The technological process for manufacturing of hydrogen pressure regulators could be evaluated by statistical analysis of the qualitative parameter roughness. Statistical analysis of stability, accuracy, and process tuning could be used for evaluation of the technological process [28].

As the requirements for surface texture have evolved, so have the standards. The most significant change in ISO 21920 [20] concerns the manner in which the calculation is conducted, it is no longer performed repeatedly and subsequently averaged. The revised calculation method entails a single value of *Ra* (or *Rq*). However, this does not apply to *Rp*, *Rv* and *Rz*, which continue to be averaged to minimize the impact of outliers [24].

5. MEASUREMENT OF SURFACE ROUGHNESS OF HYDROGEN PRESSURE REGULATORS

In a considerable number of applications, the surface texture is closely associated with the functionality of the item in its intended use, and thus affects the sealing or wear properties. The efficacy of a seal used to prevent pneumatic leaks can be influenced by the surface treatment applied. If the surface is of an excessively rough nature, it can cause wear and subsequent damage, which may result in failure [22].

In the initial phase of the hydrogen pressure regulator RH242 [11], piston displacements of approximately 0.2 to 0.4 mm can be observed, with a corresponding seal ring diameter of 0.8 to 1.2 mm. This indicates that high roughness requirements are only necessary in a specific zone of operation for the sealing elements (Figure 2).

A detailed examination of small piston movements allows the specific requirements for the macrogeometry of the surfaces and the location of the sealing rings relative to the points of extreme roughness in given areas to be determined. Figure 6 shows the principal position of the sealing ring in four different positions depending on the surface roughness, which can explain the connection with the functional requirements for hydrogen pressure regulators. It is important to note that the selection of appropriate roughness parameters may not permit a reduction in peaks, thereby ensuring effective sealing of the H_2 molecule, which is particularly small and highly aggressive. Conversely, achieving a minimum average roughness ensures protection against internal and external leaks with a low amount of sealing elements, as well as a smooth and uniform conversion characteristic.

For acquiring comprehensive texture data, the measurement of roughness will be conducted in four different directions (+*X*, -*Y*, -*X* and +*Y*) simultaneously, perpendicular to the plane of the working surfaces and parallel to the piston translation (Figure 7). The measured macro parameters can be considered to represent shape (circularity) deviations that may occur in the working section of the pneumatic cylinder in the contact zone with the sealing elements.

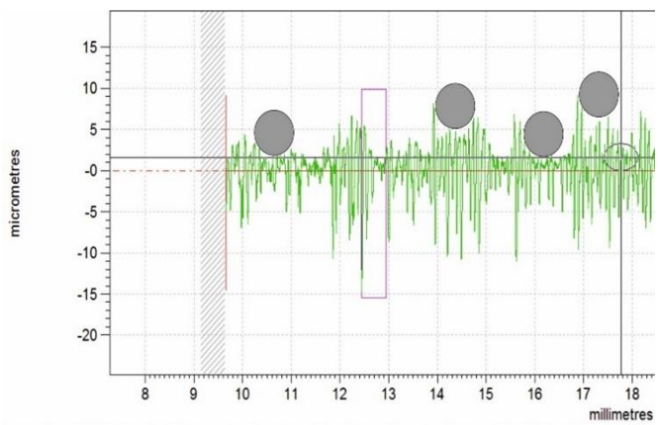

Figure 6. Different theoretical positions of the sealing ring depending on the surface texture of a roughly machined cylindrical surface measured with Taylor Hobson Form Talysurf i-series [22]

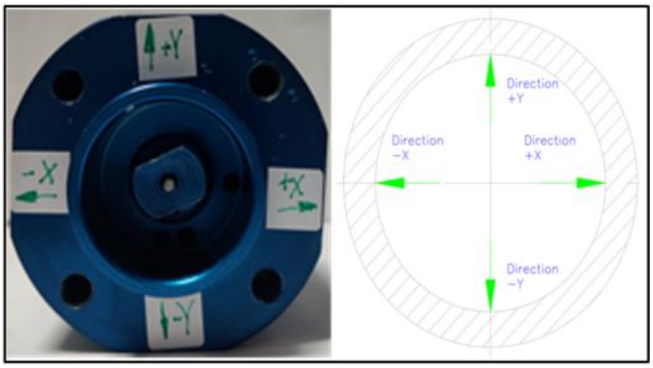

Figure 7. Directions of surface roughness measurement of Memtex RH242 parts

Figure 8. Test bench for surface roughness measurement

The surface roughness parameters are measured using the test bench shown in Figure 8. The bench includes an Insize 6900-164 granite table on which the Insize ISR-C002 Roughness Tester [29] is positioned. The position of the sensor is adjusted using an Insize Digital Height gauge 1156-300, with the components under measurement placed in a V-block. This configuration of instruments enables the sensor of the roughness tester to be aligned parallel to the cylindrical surface. The data is then processed using the dedicated software Insize DataView for Surface Roughness Tester V1.4.

The application of standard surface roughness measurement methods can be adapted for use with specific hydrogen pressure regulators. For this purpose, different statistical methods can be used to calculate average values that serve as a signal parameter for possible disturbances in the reliability of the regulators.

6. STATISTICAL ANALYSIS OF SURFACE ROUGHNESS PARAMETERS

In order to analyze the different surface roughness parameters, the results obtained by measuring the internal cylindrical surface of the first stage of the hydrogen pressure regulators Memtex RH242 [11] with the Roughness Tester INSIZE ISR-C002 [29] will be utilized. Anodized Aluminium T6511, with additional polishing of the surfaces, was used for the fabrication of the individual housing parts.

As illustrated in Figure 9, the graph presents a measurement obtained with the Insize ISR-C002 Roughness Tester [29] and displays the result for *Ra* on a cylindrical surface of a Memtex RH242 hydrogen pressure regulator. This result is presented graphically using Insize DataView software. Following the final finishing process, which involved polishing and Anodising, the surface macro geometry was characterised by the absence of sharp peaks on the roughness profile. This characteristic is of significant importance, as it ensures minimal friction between the sealing elements while providing effective hydrogen isolation from the atmosphere. The tabular representation of the findings is presented in Table 1.

Figure 9. Roughness curve displayed on Insize DataView for surface roughness tester V1.4. software

Standard measuring equipment and established techniques and methods are utilized for the analysis of surface roughness. An adapted methodology for surface roughness measurement was applied, based on an analysis of the design and technical specifics of hydrogen pressure regulators. The availability of statistical processing of the results allows for the correction to tolerances allowed, and enables rapid evaluation of process changes manifested in increased parameter variance. In contrast to popular ways of evaluating roughness measurement results, the adapted analysis methodology yields dynamically changing tolerance limits to signal potential problems.

The measurement is performed in four directions: *+X*, *-X*, *+Y* and *–Y* (Figure 7). Each measurement is repeated five times (Figure 10). In order to estimate the repeatability for each of the surface roughness parameters in the different directions, the sample mean (Eq. (9)) and the standard deviation (Eq. (10)) are calculated [30, 31].

$$\overline{R(k)} = \frac{1}{m}\sum_{j=1}^{m} R(k)_j \tag{9}$$

where, k – parameter determines the type of surface roughness calculated (*Ra*, *Rz*, *Rq*, *Rt*, *Rp*), j – consecutive number of attempts (j=1÷5), m – total number of attempts (m=5).

$$s^2_{R(k)} = \frac{\sum_{i=1}^{m}(R(k)_i - \overline{R(k)})^2}{m-1} \tag{10}$$

The calculation of the sample mean (Eq. (9)) for each roughness parameter $\overline{R(k)}$ in each of the four roughness measurement directions (see Figure 7) enables the evaluation of the process capability, particularly in the context of post-surface finish, which is of significance for hydrogen embrittlement, corrosion resistance and internal/external leakage protection. The standard deviation $s_{R(k)}$ (Eq. (10)) helps to compare the scatter of results in different measurement directions and provides a rapid estimate of random errors.

It is considered that an average value of the different roughness parameters in each direction can be used as a further estimate of the circularity deviation in the working section.

Table 1. Roughness table with measurement results of different surface roughness parameters: *Ra, Rz, Rq, Rt* and *Rp*

Measurement Direction	Roughness Parameters	1st try	2nd try	3th try	4th try	5th try
+X	*Ra*	0.59	0.492	0.638	0.635	0.504
	Rz	3.5	3.403	3.681	3.6	3.475
	Rq	0.815	0.742	0.825	0.817	0.919
	Rt	5.135	4.836	5.622	5.42	4.941
	Rp	1.1	0.976	0.983	1.014	1.16
-X	*Ra*	0.492	0.646	0.683	0.523	0.612
	Rz	3.603	3.592	3.824	3.711	3.681
	Rq	0.642	0.617	0.808	0.783	0.672
	Rt	4.736	4.361	5.529	5.105	5.265
	Rp	1.024	1.003	1.119	1.114	0.923
+Y	*Ra*	0.614	0.621	0.673	0.514	0.589
	Rz	3.923	3.987	3.805	3.782	3.839
	Rq	0.866	0.896	0.913	0.938	0.815
	Rt	4.891	4.869	5.202	4.529	5.697
	Rp	0.977	0.913	1.145	1.022	0.963
-Y	*Ra*	0.644	0.66	0.497	0.619	0.696
	Rz	4.002	3.825	4.092	3.978	3.887
	Rq	0.95	0.978	0.817	0.941	0.933
	Rt	5.664	4.714	4.861	5.265	4.714
	Rp	1.109	1.165	1.003	1.079	0.978
Average	*Ra*	0.585	0.605	0.623	0.573	0.600
	Rz	3.757	3.702	3.851	3.768	3.721
	Rq	0.818	0.808	0.841	0.870	0.835
	Rt	5.107	4.695	5.304	5.080	5.154
	Rp	1.053	1.014	1.063	1.057	1.006

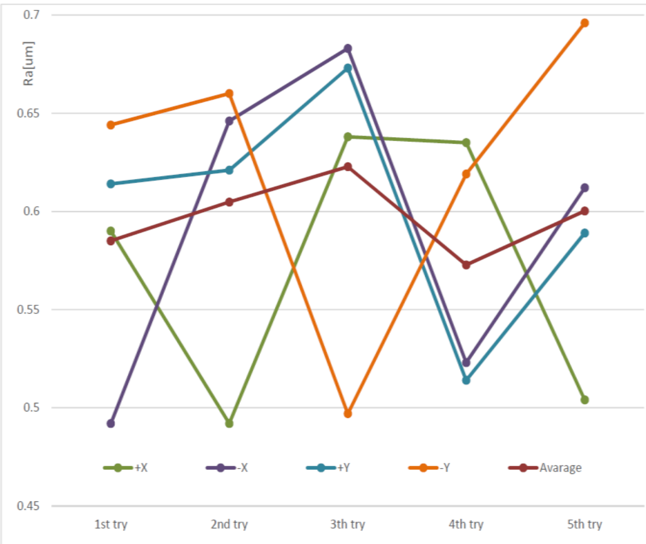

Figure 10. A scatter plot of the roughness Ra measurement in various cross-sections, with the data being derived from five separate measurements

As demonstrated in Figure 10, which presents the graphical outcomes for the surface roughness parameter *Ra*, it is evident that there is an absence of visible scatterings in the various measurement directions, with the exception of random deviations that are attributable to incorrect basing or subjective error.

A statistical evaluation of the mean values of surface roughness parameters across various cross-sections is conducted. This involves the calculation of the mean value, $R(k)_{av}$, for all cross-sections (see Eq. (11)), and the standard deviation, $s_{R(k)av}$, for all cross-sections (see Eq. (12)).

$$R(k)_{av} = \frac{R(k)_{+X} + R(k)_{-X} + R(k)_{+Y} + R(k)_{-Y}}{4} \tag{11}$$

$$s_{R(k)av} = \frac{s_{R(k)+X} + s_{R(k)-X} + s_{R(k)+Y} + s_{R(k)-Y}}{4} \tag{12}$$

In accordance with the final estimate, the maximum allowable parameters $R(k)_{lim}$ are defined on the basis of statistical analysis:

$$R(k)_{lim} = R(k)_{av} + c.s_{R(k)av} \tag{13}$$

where, *c* is the security index, which is a function of the available database and varies depending on the process and may be the manufacturer's know-how.

For the purpose of the study, we choose c=1.

According to the established methodology for the control of surface texture parameters, the measurement results obtained are compared with the tolerance limits:

$$\overline{R(k)} \leq R(k)_{tol} \tag{14}$$

In an adapted control methodology for hydrogen pressure regulators, we compare the mean parameter values with dynamically varying statistically calculated limits:

$$\overline{R(k)} \leq R(k)_{lim} \tag{15}$$

In order to evaluate the roughness parameters according to the adapted method, Eq. (15) is utilised, thereby yielding dynamically changing parameters. The results presented in Table 2 illustrate the application of statistical analysis. In the yellow cells of the table in Table 2, values of *Rz* and *Rq* are observed in the *+Y* and *-Y* directions, indicating a possible problem with shape deviation or insufficient surface stability. According to the established control methods, the parameters *Rz* and *Rq* correspond to the tolerance indicated by Equation 14. The values of the parameters *Rz* and *Rq* marked in yellow indicate elevated levels of roughness in the specified area, which has the potential to result in H_2 leaks due to material corrosion or accelerated wear of the sealing element. It is noteworthy that the elevated values are confined to two out of four measurement directions, a factor that has the potential to induce enhanced friction in these specific areas, consequently resulting in conversion characteristic unevenness.

Table 2. Roughness table with statistical parameters for surface roughness

Meas. Dir.	Roughness Parameters	Sample Mean R(k)	Standard Deviation (s)	Tolerance limit
+X	Ra	0.572	0.070	Ra≤0.8
	Rz	3.532	0.109	Rz≤4.2
	Rq	0.824	0.063	Rq≤1.2
	Rt	5.205	0.377	Rt≤6
	Rp	1.047	0.080	Rp≤3.2
-X	Ra	0.591	0.081	
	Rz	3.682	0.094	
	Rq	0.704	0.086	
	Rt	4.999	0.458	
	Rp	1.037	0.082	
+Y	Ra	0.602	0.058	
	Rz	**3.867**	0.086	
	Rq	0.886	0.047	
	Rt	5.038	0.439	
	Rp	1.004	0.088	
-Y	Ra	0.623	0.076	
	Rz	**3.957**	0.104	
	Rq	**0.924**	0.062	
	Rt	5.044	0.414	
	Rp	1.067	0.077	**R(k)lim**
Average	*Ra*	*0.597*	*0.071*	**0.668**
	Rz	*3.760*	*0.098*	**3.858**
	Rq	*0.834*	*0.065*	**0.899**
	Rt	*5.071*	*0.422*	**5.493**
	Rp	*1.039*	*0.082*	**1.120**

The applied aspect of the adapted surface roughness control methodology can be considered as an analytical tool to evaluate the performance and technical characteristics of the regulators as a function of the roughness parameters.

As the main characteristic directly influencing the performance of pressure regulators directly affecting the hydrogen fuel systems, the conversion characteristic of the input pressure Pin to the output pressure Pout is considered. This conversion characteristic is strongly influenced by the smooth and uniform movement of the piston, and this movement depends on the friction between the contact surfaces. A direct functional relationship can therefore be established between the characteristics of the surface texture and the output pressure of the regulator. Ensuring a constant regulator output pressure to the hydrogen fuel cell is the basis for its efficiency and reliable, trouble-free operation.

Another important performance characteristic that can be ensured by the developed surface roughness control methodology is related to the reliable and safe operation of hydrogen pressure regulators. Surface roughness has a direct influence on sealing element wear, which can lead to internal/external leakage. Similarly, increased roughness can lead to internal/external leakage due to the small size of the hydrogen (H_2) molecule.

In batch production, the proposed control methodology may prove cumbersome and slow. The analysis of the specific requirements and design solutions of different manufacturers, combined with their know-how, can greatly help in the adaptation and implementation of the methodology. The statistical methods applied can help to facilitate the control of the geometric dimensions and the availability of a database can facilitate the measurements and reduce the number of measurements from five repetitions in four sections to the measurement of five hydrogen pressure regulators again in four sections. This possible adaptation of the developed methodology will reduce the impact of each individual regulator on the overall evaluation through the dynamic parameter $R(k)_{lim}$, but will help to better represent the overall process and indicate changes in it in a timely manner. Another parameter that allows the possibility of enhancing and reducing the influence of process changes is c (safety index), and it largely reflects the accumulated know-how from the application of the adapted methodology to the control of surface roughness by statistical methods.

7. CONCLUSIONS

As a critical component of hydrogen systems, pressure regulators must have specific characteristics to ensure durability and reliability. Statistical analysis of surface roughness allows us to ensure production control. By dynamically changing the limits of individual parameters depending on the results obtained, we can promptly signal changes in the technological process, the signal for which is the dispersion expressed in deviations from the sample mean and standard deviation.

The applied aspect of the adapted methodology for the control of surface texture can be considered as an analytical tool for the assessment of the operability and technical characteristics of regulators as a function of roughness parameters. The developed methodology can help to overcome some of the main challenges posed by hydrogen in the manufacture and operation of pressure regulators. The conversion characteristic of the pressure regulator is directly affected by the surface roughness and has a direct impact on the efficiency and reliability of hydrogen fuel systems. To ensure safe operation, it is necessary to prevent external and internal hydrogen leaks, and due to the nature of the hydrogen molecule, very small roughness on the contact surfaces can cause such leaks.

Overcoming the technical difficulties of hydrogen pressure regulators and ensuring safe and long-lasting operation is a small step towards the possibilities of making hydrogen the green fuel of the future.

ACKNOWLEDGMENT

This research is supported by the Bulgarian Ministry of Education and Science under the second stage of the National Program "Young Scientists and Postdoctoral Students – 2".

REFERENCES

[1] OECD. (2004). Hydrogen and fuel cells. https://www.oecd.org/en/publications/hydrogen-and-fuel-cells_9789264108844-en.html.

[2] Aminudin, M.A., Kamarudin, S.K., Lim, B.H., Majilan, E.H., Masdar, M.S., Shaari, N. (2023). An overview: Current progress on hydrogen fuel cell vehicles. International Journal of Hydrogen Energy, 48(11): 4371-4388. https://doi.org/10.1016/j.ijhydene.2022.10.156

[3] De Dominicis, A. (2023). Advantages and disadvantages of green hydrogen. https://mitsidi.com/en/vantagens-e-desvantagens-do-hidrogenio-verde/.

[4] Hydrogen and Fuel Cell Technologies Office. (2014). Hydrogen fuel cell engines and related technologies course manual. https://www.energy.gov/eere/fuelcells/articles/hydrogen-fuel-cell-engines-and-related-technologies-course-manual.

[5] Chen, F.Q., Zhang, M., Qian, J.Y., Chen, L.L., Jin, Z.J. (2017). Pressure analysis on two-step high pressure reducing system for hydrogen fuel cell electric vehicle. International Journal of Hydrogen Energy, 42(16): 11541-11552. https://doi.org/10.1016/j.ijhydene.2017.02.077

[6] Chen, J., Veenstra, M., Purewal, J., Hobein, B., Papasavva, S. (2019). Modeling a hydrogen pressure regulator in a fuel cell system with Joule–Thomson effect. International Journal of Hydrogen Energy, 44(2): 1272-1287. https://doi.org/10.1016/j.ijhydene.2018.11.020

[7] Thompson, S.T., James, B.D., Huya-Kouadio, J.M., Houchins, C., et al. (2018). Direct hydrogen fuel cell electric vehicle cost analysis: System and high-volume manufacturing description, validation, and outlook. Journal of Power Sources, 399: 304-313. https://doi.org/10.1016/j.jpowsour.2018.07.100

[8] Zorpette, G. (2005). Super charged [ultracapacitors]. IEEE Spectrum, 42(1): 32-37. https://doi.org/10.1109/MSPEC.2005.1377872

[9] Ma, J., Liu, S., Zhou, W., Pan, X. (2008). Comparison of hydrogen transportation methods for hydrogen refueling station. Journal of Tongji University, 36: 615-619.

[10] EG&G Technical Services, Inc. (2004). Fuel Cell Handbook (Seventh Edition). https://www.netl.doe.gov/sites/default/files/netl-file/FCHandbook7.pdf.

[11] Hydrogen pressure regulator RH242. https://memtex.net/bg/products/components_for_gas_systems/pressure_regulators/RH242_Hydrogen_pressure_regulator_RH242.

[12] Aberlink 3D Mk4 Measurement Software - User Manual, Issue 24. https://aberlink.com/assets/public/software.

[13] Larminie, J., Dicks, A., McDonald, M.S. (2003). Fuel Cell Systems Explained. Chichester, UK: J. Wiley.

[14] ISO 11114-4:2017. (2017). Transportable gas cylinders - Compatibility of cylinder and valve materials with gas contents. https://www.iso.org/standard/64587.html.

[15] Back Pressure Regulators, BP301. https://www.pressure-tech.com/?page=product&product=56&cat=4.

[16] Sedlaček, M., Podgornik, B., Vižintin, J. (2009). Influence of surface preparation on roughness parameters, friction and wear. Wear, 266(3-4): 482-487. https://doi.org/10.1016/j.wear.2008.04.017

[17] Form Talysurf i-Series. https://www.taylor-hobson.com/-/media/ametektaylorhobson/files/product%20downloads/i-series%20range/fts-i-series_product%20brochure.pdf.

[18] ISO 4287:1997. (1997). Geometrical Product Specifications (GPS) - Surface Texture: Profile method - Terms, definitions and surface texture parameters. https://www.iso.org/standard/10132.html.

[19] ISO 1302:2002. (2002). Geometrical Product Specifications (GPS) — Indication of surface texture in technical product documentation. https://www.iso.org/standard/28089.html.

[20] ISO 21920-1:2021. (2021). Geometrical product specifications (GPS) - Surface texture: Profile. https://www.iso.org/standard/72196.html.

[21] Georgiev, K., Katsarova, P. (2024). Comparative analysis of the results of an experimental study with basic equipment and a specially made one to the in size ISR-C002 roughness tester. In Environment. Technology. Resources. Proceedings of the 15th International Scientific and Practical Conference, pp. 58-64. https://doi.org/10.17770/etr2024vol3.8106

[22] Exploring surface texture. https://www.southampton.ac.uk/~assets/doc/Engineering/exploring%20surface%20texture.pdf.

[23] Leach, R.K. (2014). The measurement of surface texture using stylus instruments. Measurement Good Practice Guide.

[24] The profile standards ISO 21920. https://guide.digitalsurf.com/en/guide-iso-21920-parameters.html.

[25] Profile Parameters from ISO 4287. https://guide.digitalsurf.com/en/guide-iso-4287-parameters.html.

[26] Gadelmawla, E.S., Koura, M.M., Maksoud, T.M., Elewa, I.M., Soliman, H.H. (2002). Roughness parameters. Journal of Materials Processing Technology, 123(1): 133-145. https://doi.org/10.1016/S0924-0136(02)00060-2

[27] Bhushan, B. (2000). Modern Tribology Handbook, Two Volume Set. CRC Press.

[28] Georgiev, K. (2024). Statistical analysis of the quality of a technological process for the production of shafts for electric motors by roughness study. In Environment. Technology. Resources. Proceedings of the 15th International Scientific and Practical Conference, pp. 70-74. https://doi.org/10.17770/etr2024vol3.8137

[29] Roughness Tester Code isr-c002.

https://www.insz.eu/user/documents/upload/drsnomery.pdf?srsltid=AfmBOopjYHQoXB1w5LFnuFFLsilbcp9N-YOKqKy3lpw8dw1UGvLSZLaq.
[30] Montgomery, D. (2011). Engineering Statistics. John Wiley & Sons, Inc.
[31] McClave, J.T., Sincich, T. (2013). Statistics. Pearson Education.

NOMENCLATURE

c	security index
D_1	first stage piston diameter, mm
F_{Pin}	pressure force on the piston of the first stage, MPa
F_{sp1}	spring force of the first stage, N
H_2	hydrogen molecule
i	consecutive number of attempts (acc. ISO 4287)
j	consecutive number of attempts
k	parameter determines the type of surface roughness calculated (Ra, Rz, Rq, Rt, Rp)
m	total number of attempts
n	total number of attempts (acc. ISO 4287)
P_1	reduced pressure from the first stage of the pressure regulator, MPa
P_2	reduced pressure from the second stage of the pressure regulator, MPa
P_{in}	inlet pressure, MPa
P_{out}	outlet pressure, MPa
ΔP	pressure reduction, MPa
Ra	roughness arithmetic mean, µm (acc. ISO 4287)
$\overline{R(k)}$	roughness parameters sample mean, µm
$R(k)_{av}$	roughness parameters average from different directions, µm
$R(k)_{lim}$	roughness parameters statistical limits, µm
$R(k)_{tol}$	roughness parameters tolerance limits, µm
$R(k)_{+X}$	roughness parameters in +X direction, µm
$R(k)_{-X}$	roughness parameters in -X direction, µm
$R(k)_{+Y}$	roughness parameters in +Y direction, µm
$R(k)_{-Y}$	roughness parameters in -Y direction, µm
Rp	roughness maximum profile peak height, µm (acc. ISO 4287)
Rq	roughness total height of the profile, µm (acc. ISO 4287)
Rt	roughness root mean square, µm (acc. ISO 4287)
Ry	roughness lowest profile valley height, µm (acc. ISO 4287)
Rz	roughness maximum height of the profile, µm (acc. ISO 4287)
s_R	roughness standard deviation, µm
$s_{R(k)av}$	average roughness parameters standard deviation from different directions, µm
$s_{R(k)+X}$	roughness parameters standard deviation in +X direction, µm
$s_{R(k)-X}$	roughness parameters standard deviation in -X direction, µm
$s_{R(k)+Y}$	roughness parameters standard deviation in +Y direction, µm
$s_{R(k)-Y}$	roughness parameters standard deviation in -Y direction, µm
S_1	piston area of the first stage, mm^2
$+X,-X$	direction of roughness measurement acc. (Figure 7).
$+Y,-Y$	direction of roughness measurement acc. (Figure 7).
y_1	moving the piston of the first stage, mm
Δy_1	relative first stage piston displacement, mm
$Z(x)$	absolute ordinate values, µm (acc. ISO 4287)